Research Article

Chemical Review and Letters
journal homepage: www.chemrevlett.com
ISSN (online): 2645-4947 (print) 2676-7279

Impact of alkalized nano-cellulose from *Calotropis gigantea* on biocomposite foam for fish freshness monitoring

Lia Handayani[1,2], Sri Aprilia[1,3], Nasrul Arahman[1,3,] *, Muhammad Roil Bilad[4]

[1]*Postgraduate School of Engineering, Universitas Syiah Kuala, Banda Aceh, 23111, Indonesia.*
[2]*Department of Fisheries Product Technology, Faculty of Fisheries, Universitas Abulyatama, Aceh Besar, 23372, Indonesia.*
[3]*Department of Chemical Engineering, Universitas Syiah Kuala, Banda Aceh, 2311, Indonesia.*
[4]*Faculty of Integrated Technologies, Universiti Brunei Darussalam, Jalan Tungku Link, Bandar Seri Begawan, BE1410, Brunei.*

ARTICLE INFO

Article history:
Received 05 June 2025
Received in revised form 10 August 2025
Accepted 24 August 2025
Available online 20 October 2025

Keywords:
Calotropis gigantea
Cellulose nanocrystals
Colorimetric indicator
Composites
Intelligent packaging

ABSTRACT

The growing demand for environmentally friendly smart packaging has driven the development of novel biopolymer-based materials that serve as food quality indicators. This study aims to evaluate the effect of different alkali agents in the production of cellulose nanocrystals (CNCs) derived from the bark of *Calotropis gigantea*, which are utilized as fillers in colorimetric biocomposite foams (BCFs) for non-destructive fish freshness monitoring. Two alkali agents, NaOH and 20% Na_2SO_3, were applied during the delignification stage prior to hydrolysis with sulfuric acid (40% H_2SO_4). The resulting CNCs were thoroughly characterized using spectroscopic, morphological, and thermal techniques. Morphological and structural analyses revealed that CNCs treated with NaOH exhibited the highest crystallinity index (89.54%) and featured shiny, needle-like crystals with a more uniform size distribution. In contrast, CNCs produced using Na_2SO_3 showed a lower crystallinity index (51.11%) with agglomerated morphology and uneven particle size distribution. The BCF formulated with CNCs-NaOH (0.25 g) exhibited a porous structure with a high specific surface area (10.64 m^2/g), which supported the immobilization of anthocyanin-based pH indicators extracted from *Clitoria ternatea*. Application testing during the storage of Oreochromis niloticus at 5 °C over 30 days showed a significant color change in the indicator, corresponding to a pH increase from 5.2 to 6.3 and a rise in TVB-N values from 2.83 mg/100 g to 32.86 mg/100 g. The CNCs-NaOH-based BCF demonstrated excellent responsiveness to environmental pH changes associated with fish spoilage. This study represents the first investigation of *C. gigantea* as a source of CNCs through varied alkali treatment approaches for use in foam-based colorimetric indicators. The findings suggest that CNCs-NaOH derived from C. gigantea show strong potential as superior fillers in responsive and sensitive porous smart packaging for real-time detection of fish freshness deterioration.

1. Introduction

As consumer demand for fresh food increases, packaging technology is evolving to meet these needs. Innovations include advancements in active and intelligent packaging, which offer enhanced functionality through improved materials and manufacturing methods. Active packaging incorporates substances such as antioxidants or antimicrobial agents to enhance the chemical and microbial stability of food. In contrast, intelligent packaging monitors the food's environment, detecting changes in its chemical composition and providing visual feedback, such as color changes [1]. These innovations offer essential information to producers, suppliers, distributors, and consumers about the freshness, quality, and safety of food products [2]. Packaging serves as a container and protector, as well as an indicator of critical changes, such as pH variations resulting from food decomposition.

Colorimetric indicators, including biocomposites like edible films and biofilms, have been extensively developed as intelligent packaging solutions. These

* Corresponding author E-mail: nasrular@usk.ac.id
https://doi.org/10.22034/crl.2025.528600.1623

materials show significant potential as indicators of food spoilage, particularly for products such as milk [3], fresh shrimp [4,5], fresh fish [6,7], and fresh meat [8–10]. The efficacy of colorimetric indicators is assessed based on their sensitivity and ability to produce a rapid color response to changes in environmental pH. However, existing biofilm-based indicators often exhibit slow color changes, typically requiring several minutes to respond [4,11,12], This makes them less suitable for applications with rapid pH fluctuations in food packaging. Innovations in porous composite-based colorimetric indicators are needed to address this limitation. These advancements aim to increase the active surface area of the indicators, enhancing their responsiveness to changes in environmental pH [13, 14]. Such enhancements could lead to more effective solutions for real-time monitoring of food freshness, thereby improving food safety and quality control.

The use of cellulose nanocrystals (CNCs) as reinforcement in composite materials aims to produce porous indicators with improved stability, porosity, responsiveness, and sensitivity to pH changes. Previous studies using microcrystalline cellulose (MCC) have shown that porous indicators can effectively detect pH variations in fresh meat and shrimp [13]. The incorporation of MCC as a filler reduced pore size, increased pore interaction, and improved porosity, thereby significantly enhancing the foam indicator's response to pH changes [13]. Similar effects were noted in studies that incorporated CNCs and cellulose nanofibers (CNFs) into a porous polyvinyl alcohol (PVA)-borax matrix [14]. Another advantage of using cellulose fibers as fillers is their ability to improve the thermal and mechanical properties of composites, as previously demonstrated with cellulose fibers extracted from banana stems [15] and from bamboo–ramie blends [16].

The physical properties of the porous indicator (biofoam) are significantly affected by the characteristics of CNCs, including their size and crystallinity. Renewable CNCs disperse effectively within the matrix, serving as both physical and chemical fillers and acting as efficient crosslinking agents during pore formation. This results in composite foams that exhibit enhanced performance, responsiveness, and sensitivity, making them excellent candidates for colorimetric indicators to monitor fish freshness. The size and characteristics of CNCs are primarily influenced by the raw materials and the manufacturing process, particularly the pretreatment stage. Pretreatment is essential for the success of the hydrolysis process, as it prepares the material for further refinement. Alkali compounds are commonly used during this stage due to their effectiveness.

The pretreatment process disrupts the lignocellulosic structure by partially breaking down its polymer components and weakening the bonds between lignin and hemicellulose. Consequently, this increases the pore size and surface area of exposed cellulose and hemicellulose, enhancing their interaction with hydrolyzing agents. Lignin and hemicellulose act as binders that reinforce cellulose fibers, making the removal of their amorphous components more challenging.

Delignification, also known as pretreatment, is an essential process that dissolves lignin in plant fibers, facilitating the separation of cellulose fibers. This is typically accomplished with chemicals such as sodium hydroxide (NaOH) and sodium sulfite (Na_2SO_3). Research indicates that sodium sulfite is more effective than sodium hydroxide in delignifying *Manihot esculenta Crantz* stems, resulting in higher yields and greater α-cellulose content [17]. The most effective delignification process involved the use of 20% Na_2SO_3 (pH = 11), yielding an α-cellulose content of 88.90%. In comparison, NaOH and Na_2SO_4 produced lower α-cellulose yields. The higher pH of NaOH (pH = 14) caused cellulose (β-cellulose) dissolution. Meanwhile, Na_2SO_4, with a lower pH (pH = 9), resulted in reduced solubility of lignin and acid detergent fiber (ADF) [17]. Among the alkali treatments, a concentration of 20% Na_2SO_3 consistently yielded the highest α-cellulose content at 88.90%, with a yield of 63.91% [17]. alpha, beta, and gamma cellulose. Alpha cellulose is the long-chain, insoluble form that resists dissolution in 16.5% NaOH solutions. Beta cellulose, on the other hand, is the short-chain form that is soluble in 16.5% NaOH. Gamma cellulose is soluble in neutral solutions and is often referred to as hemicellulose in industrial applications [18].

Various studies have demonstrated the potential of renewable biomaterials such as lignin [19], abaca fiber [20], aloe vera gel [21], and nanocellulose from agro-industrial waste as active fillers or reinforcements in biodegradable packaging [22,23]. These materials can enhance the mechanical, antibacterial, and environmental sustainability properties of poly(3-hydroxybutyrate-co-3-hydroxyvalerate) [19,20], thermoplastic starch-polyethylene [21], or pure cellulose-based materials [22,23].

These findings highlight the urgency of exploring alternative biomass sources such as *Calotropis gigantea* for nanocellulose production, optimized through alkalization processes, particularly for smart biocomposite applications in fish freshness monitoring. Coastal regions offer a variety of natural resources with significant potential for bio-composite applications, particularly the purple crown flower (*Calotropis gigantea*). CNCs derived from *C. gigantea* fibers can be utilized as effective fillers in bio-composite foams. Additionally, milkweed plants (*Calotropis* species) are known for their high cellulose content [24], The reported cellulose content ranges from 64.1% to 74.5%, lignin content from 4.4% to 9.7%, and hemicellulose is at 19.5%

[25,26], CNCs derived from *Calotropis procera*, a species related to CG, exhibit a crystallinity index of 68.7% and excellent thermal stability, indicating their suitability as reinforcement agents in the production of renewable composites [26].

The cellulose fibers derived from milkweed plants demonstrate tensile strength similar to that of cotton fibers, while exhibiting greater elongation than linen fibers. This positions them as promising sources of high-quality cellulose [25]. *C. gigantea* is an attractive option for producing CNC-based bio-composites for various applications, including eco-friendly packaging and materials.

The limited number of studies evaluating the effect of different types of alkaline agents (such as NaOH and Na_2SO_3) in the delignification process on the characteristics of cellulose nanocrystals (CNCs) derived from *Calotropis gigantea*, along with the absence of comprehensive research utilizing CNCs-CG as filler for porous foam-based colorimetric indicators in monitoring fish freshness, highlights the need for further investigation in this area. It is expected that variations in alkaline agents during delignification will produce CNCs with improved physicochemical properties, thereby enhancing the performance of the foam biocomposite as a colorimetric indicator in fresh fish packaging.

This study introduces several novel contributions: (1) the utilization of CNCs derived from *Calotropis gigantea*, a non-conventional cellulose source, as filler in foam biocomposites for colorimetric indicators, (2) a comparative investigation into the influence of two alkaline agents (NaOH and Na_2SO_3) on the resulting CNCs characteristics, including crystallinity, particle size, and thermal stability, and (3) the direct application of the resulting composite in fish packaging to monitor freshness through changes in pH and total volatile basic nitrogen (TVB-N) levels thereby bridging laboratory scale research with practical needs in the food industry.

The main objective of this research is to synthesize CNCs from the stem bark of *Calotropis gigantea* using two different alkaline treatments (NaOH and Na_2SO_3), and to apply the CNCs as fillers in biocomposite foam intended to serve as a colorimetric indicator. The CNCs will be characterized by their functional groups using Fourier Transform Infrared (FTIR) spectroscopy, crystallinity index using X-ray Diffraction (XRD), and particle size distribution using a Particle Size Analyzer (PSA).

Morphological properties will be examined using Scanning Electron Microscopy (SEM) and Transmission Electron Microscopy (TEM), while thermal stability will be analyzed using Thermogravimetric Analysis (TGA) and Derivative Thermogravimetry (DTG). Fish freshness parameters will be assessed based on pH value and total volatile basic nitrogen (TVB-N) content, analyzed using the Conway microdiffusion method.

2. Materials and Methods

2.1. Materials

The primary material used was fiber extracted from the stem bark of the purple crown flower (*C. gigantea*). Only mature stems were selected, as previous studies indicated that they provide optimal results [27]. They were Sulfuric acid (H_2SO_4, p.a., Merck), Sodium sulfite (Na_2SO_3, Merck), Sodium hydroxide (NaOH, p.a., Merck), Distilled water, Hydrogen peroxide (H_2O_2, Merck), Trichloroacetic acid (TCA, pro analysis grade), Boric acid (H_3BO_3, p.a., Merck), Indicator solution (methyl red and bromocresol green), Hydrochloric acid (HCl, p.a., 37% (v/v)), Ethanol (C_2H_6O, p.a., 96% (v/v), Merck), Polyvinyl alcohol (PVA, Mw 9,000–10,000; 80% hydrolyzed), Polyvinylpyrrolidone (PVP, Mw 40,000), Anthocyanins from butterfly pea flower extract, Crystalline sugar, Freshly caught Nile tilapia (*Oreochromis niloticus*) from aquaculture ponds at the Faculty of Fisheries, Universitas Abulyatama, Aceh, Indonesia.

2.2. Preparation of Cellulose Nanocrystals (CNCs)

2.2.1. Pretreatment of CNCs

The process began with water retting, during which purple crown flower stems were collected from the coastal area of Gampong Tibang in the Syiah Kuala District of Banda Aceh City. The stems were air-dried for one week and then soaked in water for four days. Following the retting phase, the pulping stage commenced with the peeling of the stem bark of *C. gigantea* (CG) and the separation of the fibers from the outer bark.

The fibers were subsequently washed and dried. Delignification was performed using two alkali treatments: 20% sodium hydroxide (NaOH) and 20% sodium sulfite (Na_2SO_3). The fibers were refluxed in a 20% NaOH solution (1:10 w/v) for two hours at 90°C, then thoroughly washed and neutralized to pH using dilute acetic acid. A second treatment was applied using Na_2SO_3. After delignification, the fibers were bleached with a mixture of 5% hydrogen peroxide (H_2O_2) and 3.8% NaOH (1:1 v/v). The bleaching process involved refluxing the fibers (1:20 w/v) for two hours at 90°C, followed by drying at 105°C until a constant weight was achieved.

2.2.2. Acid Hydrolysis

CNCs were produced via acid hydrolysis. Fibers treated with NaOH and Na_2SO_3 during the delignification stage underwent hydrolysis with 40% sulfuric acid (1:20 w/v) for 3 hours at 80°C. The resulting solution was filtered, neutralized with distilled water, and dried at 40°C until a constant weight was reached. The dried

material was then refined by passing it through a 325-mesh sieve.

2.3. CNCs Biocomposite Foam (BCF)

The preparation of biocomposite foams (BCF) was adapted from a previous study [13]. A mixture of 1 g of polyvinyl alcohol (PVA) and 0.2 g of polyvinylpyrrolidone (PVP) was prepared in 10 ml of distilled water and sonicated using an ultrasonic irradiator (Sonics-Vibra Cell VCX 750). After thorough mixing, 0.25 g and 0.50 g of CNCs obtained from both the NaOH and Na_2SO_3 delignification stages were added, along with a control sample without CNCs.

The mixture was sonicated again and poured into a petri dish, where 20 g of sugar crystals were manually stirred in. After mixing, the solution was frozen for 24 hours and then stored at room temperature for an additional 48 hours to facilitate cross-linking reactions between the PVA and PVP matrices. The resulting gel was washed with water at 50°C to remove unreacted sugar and then cut into square-shaped samples. The BCF samples were labeled as follows: T1 (0.25 g CNCs from the NaOH treatment), T2 (0.25 g CNCs from the Na_2SO_3 treatment), and T0 (the control without CNCs).

2.4. Preparation of Indicator

BCF samples (T0, T1, and T2) with optimal surface area and morphology were selected for processing into a colorimetric indicator. These samples were immobilized using anthocyanin extracted from butterfly pea flowers. The BCF samples were immersed in 20 ml of butterfly pea flower extract for 24 hours. The extract was prepared by diluting 4 ml of concentrated extract with 20 ml of distilled water. Following immobilization, the anthocyanin-treated BCF samples were freeze-dried for 24 hours, making them suitable for use as colorimetric indicators in intelligent packaging.

The anthocyanin extract from butterfly pea flowers was obtained using a previously established method [28]. Fresh butterfly pea flowers were extracted using a 96% ethanol solution at a 1:4 weight-to-volume ratio, combined with 1.5 N HCl at a 99:1 volume ratio.

2.5. Trial of Biocomposite Foam Response as a Colorimetric Indicator

2.5.1. Respons to Fish Freshness

Tilapia fish, cleaned and in a pre-rigor state, were placed in a beaker with a colorimetric indicator. The beaker was covered with plastic wrap and stored in a refrigerator at 5°C. Observations were conducted at intervals of 0, 5, 10, 15, 21, and 30 days, focusing on changes in indicator color, pH, and total volatile basic nitrogen (TVBN) levels.

2.6. Characterization of CNCs, Biocomposite Foam, and Fish Freshness Measurement

2.6.1. Functional Group Analysis

CNC samples were analyzed using FTIR to examine structural and functional group changes at each treatment stage. The purpose of this analysis is to determine whether lignin or other impurities are still present in the CNCs produced. This is achieved by identifying the functional groups associated with these compounds. Functional group analysis is crucial for verifying the purity of CNCs, as the presence of residual lignin or other contaminants can affect their performance in applications. By detecting specific functional groups, the analysis provides insight into the chemical composition and confirms the effectiveness of the extraction and purification processes.

The analysis was performed with an FTIR instrument (IRPrestige-21, Shimadzu, Kyoto, Japan) over a wavelength range of 4000 to 400 cm^{-1}. The samples were homogenized with potassium bromide (KBr) and pressed into transparent pellets prior to analysis.

2.6.2. Investigation of Crystallinity Index

The crystallinity of the CNCs at each treatment stage was tested using X-Ray Diffraction (XRD). The crystallinity index (CrI) was calculated using the following equation:

$$\mathrm{CrI} = \frac{\mathrm{I_{002}} - \mathrm{I_{am}}}{\mathrm{I_{002}}} \mathrm{x}\ 100\% \quad (1)$$

Where I002 is the intensity of the highest peak corresponding to the crystalline material with a Miller index (002) at a 2θ angle range of 22–23°, and Iam is the minimum diffraction intensity of the amorphous material, taken around 18° at the valley between the peaks, representing the amorphous content in the cellulose fibers [29].

The crystallite size was calculated using the Scherrer equation:

$$\mathrm{L} = \frac{\mathrm{K}.\lambda}{\beta_{\frac{1}{2}} \cos\theta} \quad (2)$$

Where L is the crystallite size (nm), K is the Scherrer constant (0.91), λ is the X-ray wavelength, β1/2 is the full width at half maximum (FWHM) of the diffraction peak, and θ is the Bragg angle.

2.6.3. Thermogravimetric Analysis (TGA)

The thermal properties of the samples were analyzed using TGA (Shimadzu DTG-60, Kyoto, Japan). A 15.300 mg sample was heated from 25°C to 600°C at a constant rate of 10°C per minute under vacuum conditions.

2.6.4. Morphological Analysis

The morphological analysis of CNCs in this study utilized two electron microscopy techniques: transmission electron microscopy (TEM) and scanning electron microscopy (SEM).

Each technique offers distinct advantages, making it necessary to employ both for comprehensive data acquisition. SEM provides information on the surface condition and composition of CNCs, while TEM delivers invaluable insights into the internal structure of the sample, including crystal structures, morphology, and structural defects or impurities.

The primary advantage of SEM is its ability to produce 3D images of the sample surface, whereas TEM generates 2D projections of the sample. On the other hand, TEM excels in achieving magnifications of up to 500,000x and a resolution as high as 0.2 nm, enabling direct visualization of crystal lattices and internal defects within the sample.

The surface morphology of the samples was analyzed using scanning electron microscopy (SEM; JSM-6360LA, JEOL Ltd., Tokyo, Japan). To enhance conductivity, the samples were coated with a thin layer of gold, and the analysis was conducted at an acceleration voltage of 1-14 kV. The JEOL TEM 1400, capable of achieving a resolution of up to 0.2 nm, was utilized for transmission electron microscopy. The operating voltage was set to 120 kV, with magnification levels ranging from 200x to 1,200,000x.

2.6.5. Surface Area

Surface area and pore volume were analyzed using a Quantachrome Corporation instrument with NOVA Data Analysis Package Ver. 2.00 software. Prior to measurement, the sample was degassed with helium at 205°C for 30 minutes. Measurements were conducted based on the number of nitrogen molecules absorbed by the sample at 77 K. The specific surface area was calculated using the BET equation, and pore volume data were determined using the BJH equation.

2.6.6. Measurement of pH and Volatile Amine

The analysis of pH and Total Volatile Basic Nitrogen (TVBN) levels in the samples was conducted to assess the degree of fish spoilage.

These parameters serve as key indicators of fish freshness, with changes in pH and elevated TVBN levels reflecting biochemical and microbial degradation processes. This analysis is critical for evaluating the quality and safety of the fish samples. The pH and Total Volatile Basic Nitrogen (TVBN) levels were measured according to established procedures from a previous study [27].

3. Results and discussion

3.1. Characteristics of CNCs-CG

3.1.1. FTIR

FTIR was used to identify the functional groups in the CNC samples. Figure 1 displays the functional groups of the fibers, cellulose, and CNCs extracted through various alkali treatments, based on spectra in the wavelength range of 500–4000 cm^{-1}. The absorption peaks at approximately 3400 cm^{-1} and 2900 cm^{-1} correspond to the stretching of OH and CH bonds in the aliphatic groups of polysaccharides [26]. The sharper and more intense peaks observed in the CNC spectra of samples c and e indicate a higher cellulose content compared to the untreated fibers and those that underwent the delignification process. This suggests that the sulfuric acid hydrolysis used in CNC production effectively degraded both lignin and hemicellulose structures.

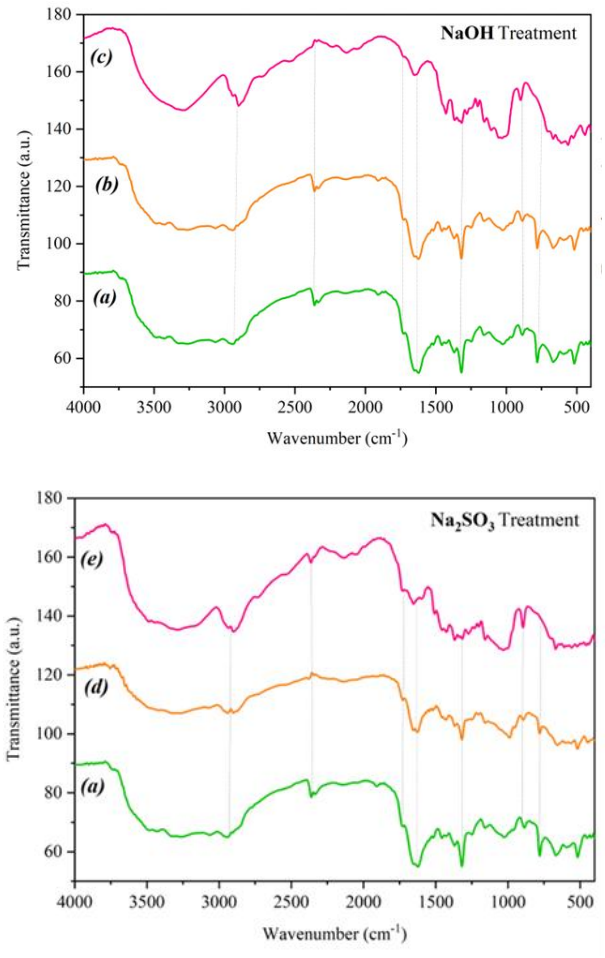

Fig. 1. Spectra FTIR: for raw material/ after water retting (a); Cellulose after delignification (b, d); CNCs (c, e).

Absorption peaks in the wavelength range of 1700–1300 cm^{-1} indicate the presence of lignin and hemicellulose. For the fiber and cellulose samples (a, b, d), the intensity and sharpness of the peaks suggest a high

content of these impurities. This finding aligns with previous studies, which indicate that delignification alone is often ineffective in removing lignin. However, subsequent bleaching is more effective, particularly for fibers from older *C. gigantea* stems [27]. Older *Calotropis* stems have higher gum content. The bleaching process involves a mixture of 3.8% NaOH and 5% H_2O_2, along with heating, to eliminate residual impurities such as pectin, lignin, hemicellulose, ferulic acid, and p-coumaric acid. While hemicellulose is not soluble in water, it is soluble in dilute alkali.

The peaks in the 1700–1300 cm^{-1} range, which indicate the presence of lignin and hemicellulose, exhibit lower intensity and sharpness in samples treated with Na_2SO_3 compared to those treated with NaOH. This finding suggests that Na_2SO_3 is less effective at lignin removal than NaOH. Research indicates that the optimal delignification process involves using Na_2SO_3 at a concentration of 20% (pH = 11), yielding an α-cellulose content of 88.90%. This makes Na_2SO_3 more effective at degrading lignin than both NaOH (pH = 14) and Na_2SO_4 (pH = 9) [17]. After bleaching, the lignin content in the Na_2SO_3-treated sample (c) significantly decreased compared to the NaOH-treated sample (e). This difference contributes to the higher crystallinity index observed in the CNCs treated with NaOH, as confirmed by the XRD analysis (Table 1). The characteristics of cellulose fibers are highly influenced by alkali concentration, temperature, and processing time. Excessively high alkali concentrations and temperatures, as well as prolonged processing times, can damage the cellulose structure. Conversely, very low alkali concentrations and temperatures, along with short processing times, lead to low cellulose yield due to the high residual content of hemicellulose and lignin.

3.1.2. XRD

The XRD diffractograms of fibers, cellulose, and CNCs, whether delignified with NaOH or Na_2SO_3, exhibit similar characteristics, featuring two primary peaks corresponding to the amorphous and crystalline phases (Figure 2). The amorphous phase is indicated by a weak diffraction peak at 2θ around 18° (Iam), while the crystalline phase shows prominent peaks at 2θ angles related to crystallographic planes: 101 (approximately 13-14°), 10i (around 15°), and 002 (approximately 22-23°). Additionally, a lower-intensity diffraction peak is observed at 040 (around 34-35° 2θ). These peak positions align with those reported in previous studies on fibers from *C. gigantea* young bark, old *C. gigantea* bark, and *C. gigantea* fruit fibers [27]. Similar findings have been reported by other researchers, who identify the amorphous peak typically within the 2θ range of 17-18° [26,30–32].

The diffractograms for cellulose (samples b and d) show peaks indicative of a crystalline phase, with greater intensity than those observed in the fibers (sample a). This suggests that the alkalization (delignification) process utilizing alkali (NaOH and Na_2SO_3) has effectively degraded portions of the lignin structure. In the diffractogram of the fibers (sample a), the peaks observed at specific crystallographic angles correspond to the retting stage, a pre-treatment process also known as degumming, which has removed some lignin. This finding is further corroborated by the FTIR spectra presented in Figure 1. These results are consistent with previous studies on the performance of *C. gigantea* fibers from various parts of the plant [27]. The use of Na_2SO_3 effectively removes lignin while preserving α-cellulose, achieving a higher degree of crystallinity at 67.32%, compared to 47.38% in samples not treated with Na_2SO_3 [33].

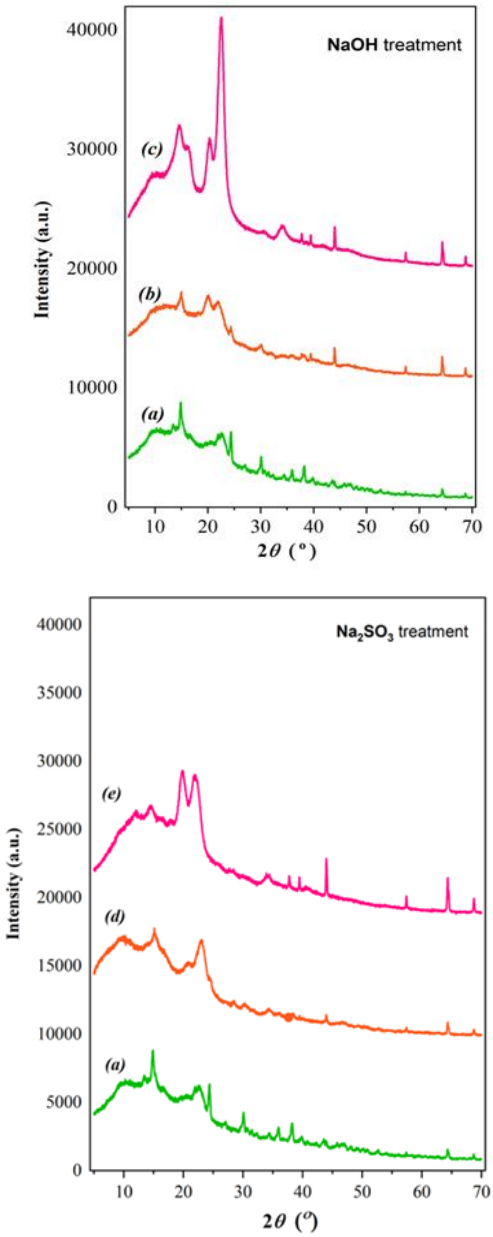

Fig. 2. Spectra XRD: for raw material/ serat after water retting (a); Cellulose after delignification (b, d); CNCs (c, e).

In contrast to the diffractograms of fibers and cellulose, the CNCs display sharply defined peaks indicative of the crystalline phase, particularly for those delignified with NaOH. A significant peak at the 2θ value of 22.6° indicates high intensity, suggesting that NaOH is more effective in removing lignin and hemicellulose, which enhances the hydrolysis process for CNC production compared to Na_2SO_3. Effective lignin removal results in a higher degree of crystallinity due to the more complete elimination of amorphous regions. CNCs treated with NaOH achieve a crystallinity index of 89.54%, while those treated with Na_2SO_3 reach 51.11%. These indices exceed the 68.7% crystallinity of CNCs derived from *C. gigantea* fruit [26], *C.gigantea* stem at 39.8% [32], and *C.gigantea* bark at 83.2% [34]. The differences in crystallinity indices are significantly influenced by the production process, particularly during lignin removal stages such as degumming, alkalization, bleaching, and acid hydrolysis. Additionally, factors such as time, solvent type, and concentration also play a critical role.

3.1.3. Particle size of CNCs

The particle size distribution of CNCs produced with different alkalis is shown in the histogram in Figure 3. CNCs produced with NaOH exhibit a more uniform particle size compared to those made with Na_2SO_3. The Na_2SO_3 salt results in cellulose particles that are smaller and more evenly dispersed. Delignification with Na_2SO_3, or sulfonation, modifies the hydrophilic properties of lignin by introducing sulfonate groups, which are more polar than the hydroxyl groups in lignin. This process enhances the hydrophilicity of lignin, converting it into lignosulfonate.

Previous studies have shown that salts like NaCl, $NaSO_4$, and $(NH_4)_2SO_4$ produce cellulose particles smaller than 1 µm, while $ZnSO_4$ and $ZnCl_2$ result in larger particles exceeding 1 µm This aligns with findings that indicate Na_2SO_3 produces higher cellulose yields than NaOH [17]. The combination of NaOH and Na_2SO_3 solutions yields cellulose particles with an average size of 55.19 µm and a diameter of 8.12 µm. In contrast, cellulose produced without Na_2SO_3 exhibits larger particle sizes, averaging 155.91 µm with a diameter of 52.95 µm [33]. ANOVA testing confirms that Na_2SO_3 significantly affects the size of cellulose produced from barley straw [35].

3.1.4. Morphological investigations

Scanning Electron Microscopy (SEM) was utilized to investigate the surface structure of fibers, cellulose, and CNCs subjected to alkali treatment with sodium hydroxide (NaOH) and sodium sulfite (Na_2SO_3). SEM images of the raw material show fibers coated with impurities that create a rough and uneven surface. These impurities include lignin, hemicellulose, and wax (Fig. 5a). Lignin, which provides structural support to the fibers, is not entirely removed during the retting process, leaving it still enveloping the fibers. In contrast, fibers subjected to delignification show disrupted lignin bonds, resulting in a clearer exposure of the fibers (Figure 4b; 4e). However, some lignin and other impurities persist, as indicated by the still rough and uneven cellulose surface (Figure 4b; 4e). This persistence of impurities following delignification is corroborated by FTIR functional group analysis (Figure 1b; 1d). Notably, fibers treated with Na_2SO_3 (Figure 5e) exhibit a cleaner surface compared to those treated with NaOH (Figure 4b), supporting previous findings that Na_2SO_3 is more effective at lignin removal [17,33,35,36].

Table 1. Crystallinity and crystallinity orientation index of CNCs

Samples	CI (%)	2*θ* (101) (º)	2*θ* (10i) (º)	2*θ* (am) (º)	2*θ* (200) (º)	Crystallite size (nm)
A	89.54	13.9	14.6	18.3	22.6	1.55
B	51.11	13.2	14.7	18.2	22.3	1.62

(A) CNCs-NaOH treatment; (B) CNCs-Na2SO3 treatment

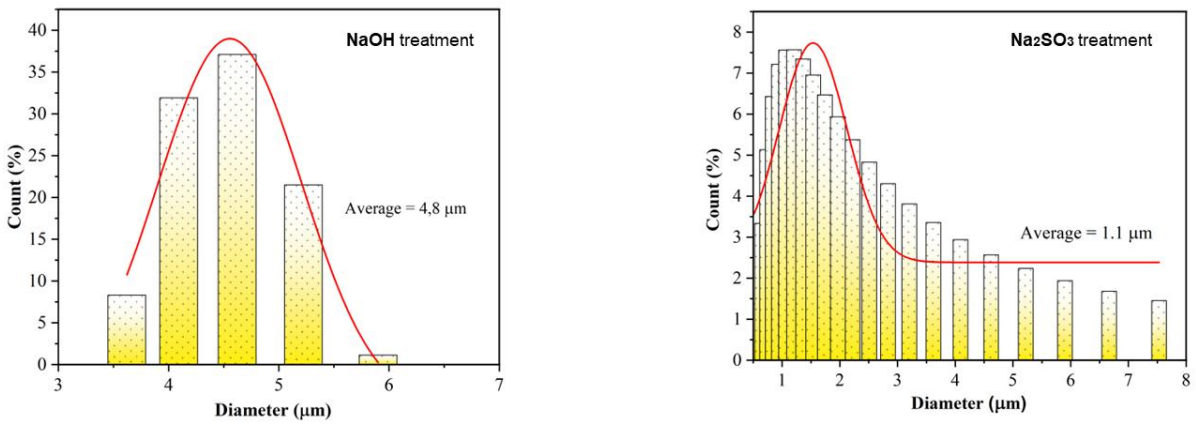

Fig. 3. Size distribution of CNCs

These results are consistent with previous studies, which indicate that delignification alone is insufficient for completely removing lignin and other impurities. Subsequent bleaching stages are essential for eliminating residual impurities [27]. Bleaching treatment using a mixture of H_2O_2 and NaOH effectively eliminated residual impurities from the delignification stage, resulting in smoother and cleaner surfaces for both cellulose samples (Figure 4c; 4f), particularly for the cellulose treated with Na_2SO_3. This enhancement in surface smoothness (Figure 5f) is consistent with previous studies indicating that the combination of NaOH, an ionic solution like Na_2SO_3, and a bleaching agent is significantly more effective in removing lignin and other extractives compared to combinations that do not include Na_2SO_3 [33,37,38]. While each delignification and bleaching stage has its benefits and limitations, the hydrolysis stage is also essential for producing CNCs. CNCs produced with NaOH exhibit larger particle sizes and a shinier, needle-like appearance (Figure 4d) compared to those treated with Na_2SO_3 (Figure 4f). This difference is reflected in the crystallinity index, with NaOH-treated CNCs showing a crystallinity of 89.54%, while Na_2SO_3-treated CNCs have a crystallinity of 51.11% (Tab. 2). Particle size analysis (PSA) (Figure 3) reveals that Na_2SO_3 treatment results in smaller and less uniformly distributed particles, in contrast to the more uniform particles obtained from NaOH treatment. SEM analysis shows that NaOH-treated CNCs form long, shiny, needle-like structures, whereas Na_2SO_3-treated CNCs appear smoother but more clumped. Hydrolysis with H_2SO_4 causes the breakdown of cellulose into shorter crystals, disrupting hydrogen bonds and resulting in smaller CNCs. The removal of the amorphous phase due to prior delignification further contributes to the formation of smaller microfibrils. The SEM morphological results align with the TEM analysis (Figure 5). The images indicate that CNCs produced with Na_2SO_3 exhibit greater agglomeration and smaller particle sizes than the more defined and robust morphology of CNCs produced with NaOH. This is further corroborated by the higher crystallinity index of the NaOH-treated CNCs, indicating a superior crystalline structure compared to the Na_2SO_3-treated CNCs. Under electron beam imaging, CNCs (Figure 5a) appear more transparent compared to the NaOH-treated CNCs.

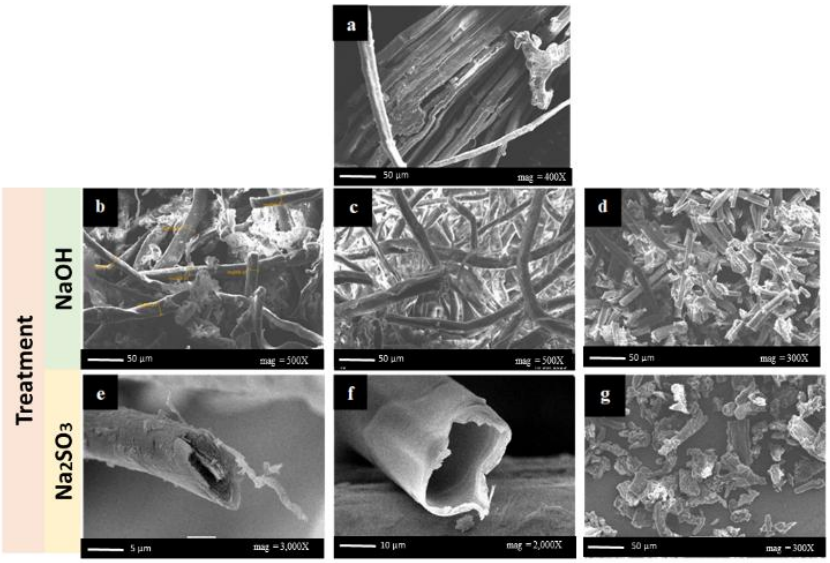

Fig. 4. SEM image: for raw material/Calotropis fiber (a); Cellulose after delignification (b, e); Cellulose after bleaching (c, f); CNCs (d, g)

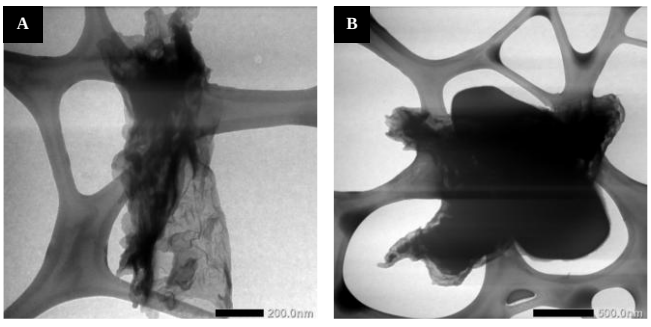

Fig. 5. TEM image, CNCs with Na_2SO_3 treatment (a), CNCs with NaOH treatment (b).

3.1.5. TGA

The TGA and DTG curves for fibers, cellulose, and CNCs derived from the bark of *C. gigantea* are analyzed over a temperature range of 20 to 600°C (Figure 6). The decomposition of these samples occurs in three distinct stages. The first stage, occurring between 30 and 110°C, represents the evaporation of bound water. The second stage, from 180 to 350°C, involves the thermal decomposition of organic compounds. Hemicellulose decomposes between 180 and 280°C, while cellulose fully decomposes between 280 and 350°C [39]. The high molecular weight and extensive hydrogen bonding in cellulose lead to strong interactions among its components, resulting in greater thermal stability compared to hemicellulose. The third stage of thermal degradation is carbonization, which occurs between 360 and 600°C. At temperatures ranging from 360 to 400°C, the breaking of C-C and C-O bonds indicates the degradation of lignin. Lignin, characterized by its aromatic structure, is located within the microfibrils between the amorphous and crystalline regions of cellulose. Lignin decomposition continues beyond 400°C and is complete by 500°C, with carbon formation observed as residue by 600°C. This decomposition process generates carbon monoxide (CO), carbon dioxide (CO_2), water (H_2O), and charcoal. This analysis underscores the thermal behavior of cellulose, hemicellulose, and lignin, as well as their respective stabilities at elevated temperatures.

The thermal degradation onset (Tonset) of the raw material occurs at 314°C, earlier than that of the CNCs treated with Na_2SO_3 or NaOH. This earlier onset is due to the high concentration of impurities in the raw material, including hemicellulose, lignin, and other organic compounds, which decompose at higher temperatures than the CNCs, which degrade within the range of 410-425°C. The thermal degradation of the raw material (bark fiber from *C. gigantea*) results in a significant residue of 31.43%, indicating a high content of hemicellulose, cellulose, lignin, and other organic substances. This finding aligns with other studies, such as those on fibers from *Typha domingensis*, which reported a residue of 30.70% [40].

Maximum weight loss for all samples occurs between 314°C and 435°C, closely associated with the degradation of cellulose I and α-cellulose [41]. The incorporation of CNCs as fillers in the composite exhibits thermal behavior that closely resembles the inherent thermal properties of CNCs, as previously described and investigated by researchers [42]. The maximum weight loss in *Calamus manan* fibers occurs between 280°C and 360°C [43]. In this study, CNCs demonstrate a lower residue of 13-18% compared to other reports, which indicate residues of 18-25% [44], 17.35% [43], and 14-20% [37]. Cellulose pyrolysis is theoretically expected to yield 44.4% carbon residue, assuming complete removal of hydrogen and oxygen as water (H_2O) through dehydration (Table 2).

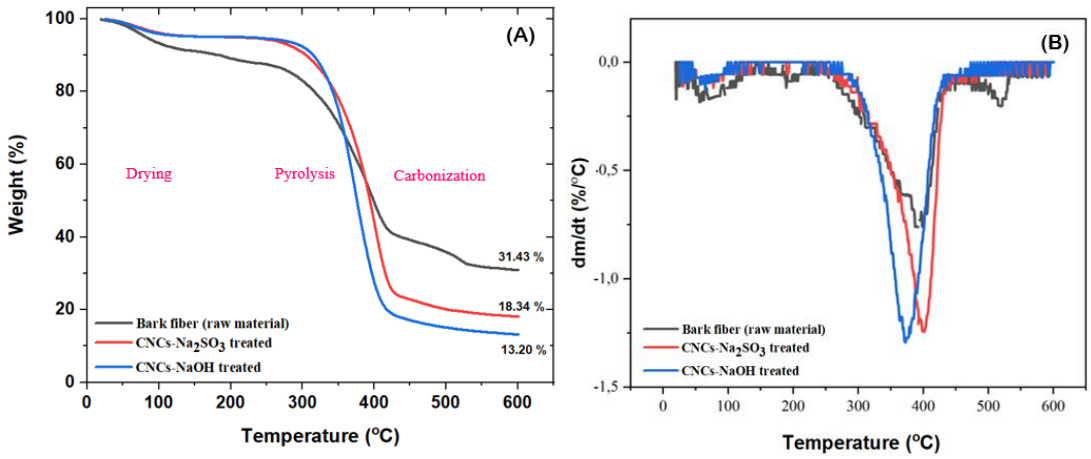

Fig. 6. (A) TGA and (B) DTG spectra of fiber (raw material) and nanocrystalline cellulose with various alkali treatment

Table 2. Crystal size, Crystalinity index and starting termal degradation

Sample	XRD		TGA		
	Crystalite size (nm)	CI (%)	Starting thermal degradation (°C)	Ending thermal degradation (°C)	Residues after 600°C (%)
CNCs-NaOH treatment	1.55	89.54	333	410	13.20
CNCs-Na_2SO_3 treatment	1.62	51.11	347	425	18.34
Bark fiber	-	31.02	314	435	31.43

However, this process involves additional complex reactions, including decarboxylation to carbon dioxide (CO_2), decarbonylation to carbon monoxide (CO), and the production of gases such as hydrogen (H_2) and methane (CH_4) [44,45].

The higher maximum degradation temperature of CNCs compared to raw bark fiber is attributable to the greater ash content in the untreated material, which serves as a catalyst during pyrolysis and accelerates cellulose degradation.

3.2. Characteristics Biocomposite Foam

3.2.1. SEM

The incorporation of CNCs as fillers in foam composites for colorimetric indicators in fish freshness monitoring significantly influences their morphological properties. This effect is evident in the pore formation observed in the composites (Figure 7), which are presented at magnifications of 100x, 50x, and 35x. Although pore formation appears similar across samples, morphology T1 exhibits superior results, characterized by a greater number of pores. This finding is supported by surface area measurements obtained through the BET method (Figure 8 and Table 3). The composite containing NaOH-treated CNCs (T1) shows enhanced pore formation, particularly at 100x and 35x magnifications. This improvement in pore structure is linked to the higher crystallinity index of the CNCs used (Table 1) and their functional groups (Figure 1). Previous studies indicate that fillers with lower lignin content and higher crystallinity indices contribute to superior composite morphology [27].

The interaction between the matrix and filler in a composite results in a porous morphological structure. In this study, hydrogen bonds are established between the hydroxyl groups of the PVA matrix and those of the CNC filler. These bonds stem from intermolecular interactions between polar covalent compounds with significant differences in electronegativity, leading to strong dipole interactions. Hydrogen bonds typically occur in compounds that contain hydrogen atoms bonded to highly electronegative elements such as fluorine, oxygen, nitrogen, or chlorine. The strength of potential hydrogen bond formation increases with the electronegativity of the atom bonded to hydrogen.

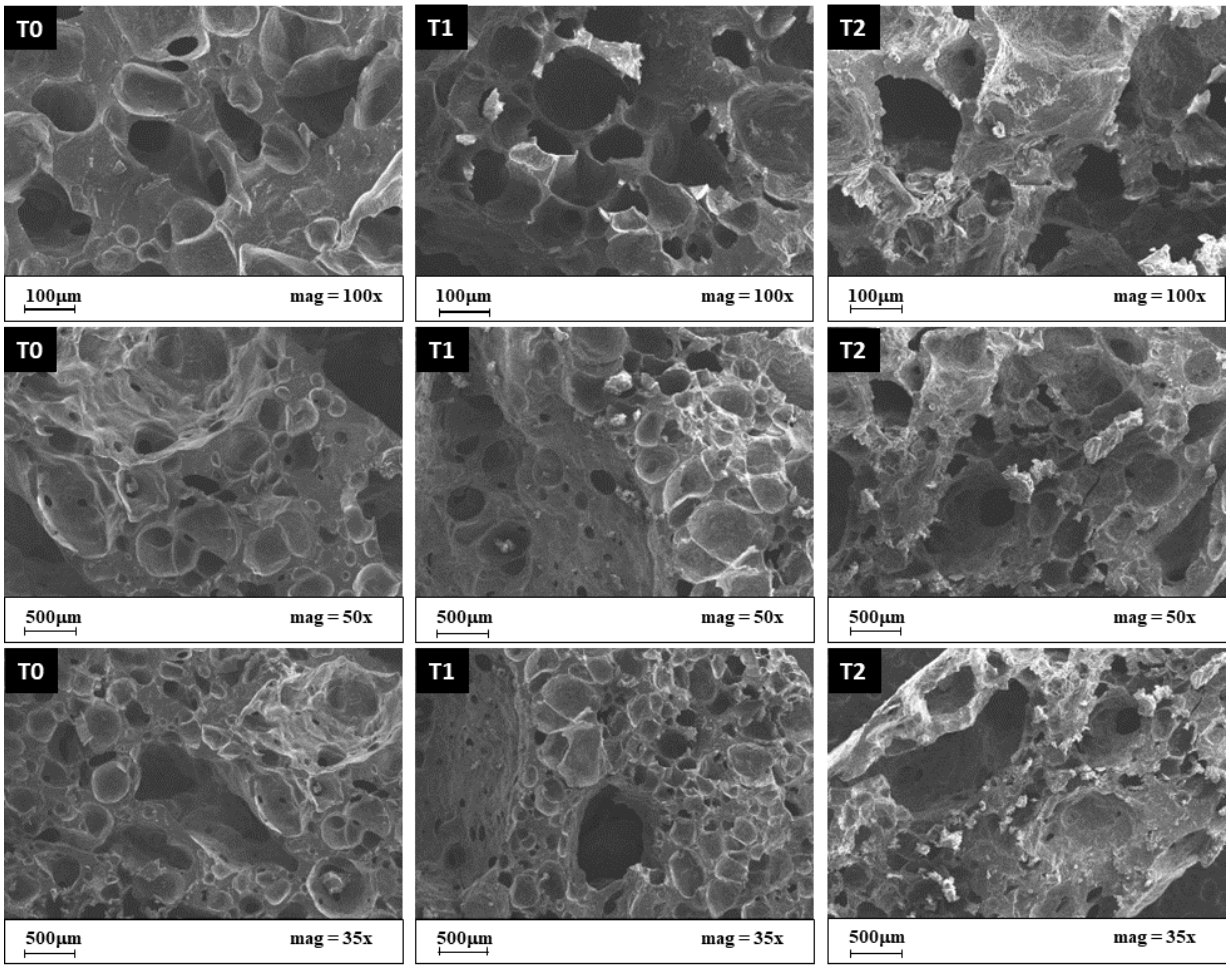

Fig. 7. Morphology of biocomposites with added CNCs; surface image of (T0) control, (T1) BCF/CNCs-NaOH treated, (C) BCF/CNCs-Na_2SO_3 treated

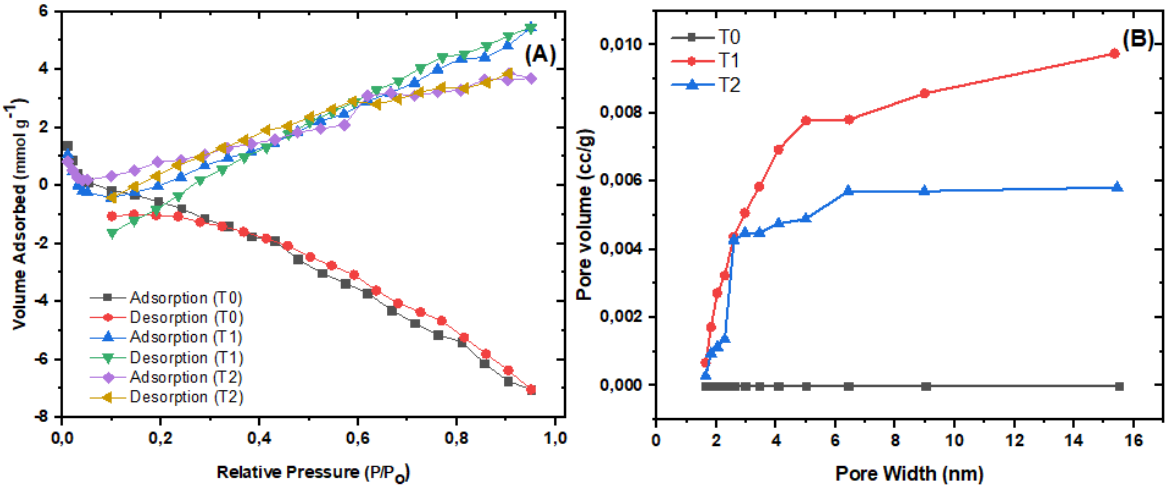

Fig. 8. N_2 adsorption and desorption isotherms recorded at 77.3 K; (B) pore size distributions of composite

Table 3. Multi BET Analysis

Properties	**T0**	**T1**	**T2**
Specific Surface area BJH (m^2/g)	0.000	6.424	4.314
Pore volume (m^2/g)	0.000	0.010	0.006
Average pore Diameter or size BJH (nm)	-0.00489	0.0158	0.0167
BET summary surface area (m^2/g)	0.445	10.639	6.834
BET pore Diameter (nm)	1.634	1.816	2.582
Correlative Coefficient	0.917	0.668	0.805

Cellulose with a higher degree of crystallinity offers enhanced dimensional stability and improved accessibility as a filler in composites. This aligns with prior research indicating that composites incorporating cellulose fibers with higher crystallinity display superior morphology [27]. Studies have demonstrated that incorporating MCC into a PVA/PVP matrix enhances porosity and pH sensitivity, resulting in these composites being effective colorimetric indicators for monitoring meat freshness [13].

3.2.2. Surface Area

Nitrogen adsorption-desorption characterization was performed to evaluate the surface area and pore size of the composites using the BET (Brunauer-Emmet-Teller) method, with nitrogen gas as the adsorbate. The resulting data, illustrated in Figure 8, is presented as isotherm curves that plot the volume of N_2 adsorbed and desorbed against the relative pressure (P/P_0). Figure 8.A indicates that the isotherm curves are of type IV, which, according to IUPAC classification, suggests the presence of pores ranging from 1.5 to 100 nm.

At higher pressures, the curve's slope reflects increased adsorbate uptake as the pores fill, with an inflection point typically occurring at the completion of the first monolayer. This type IV isotherm confirms mesoporous characteristics, with nitrogen adsorption observed in the monolayer pores of composites T1 and T2 at relative pressures below 1 ($P/P_0 < 1$). For composite T2, saturation of gas adsorbate filling occurs at relative pressures between 0.6 and 1.0. In contrast, composite T1 continues to exhibit increased N_2 adsorption at these pressures, with adsorption rising steadily from low pressures below 0.2 ($P/P_0 < 0.2$) up to $P/P_0 = 1$ within the mesopores. The volume of adsorbed gas stabilizes once all available surfaces are covered by the adsorbate, as seen for composite T2 ($P/P_0 = 0.6$-1.0). This indicates that composite T2 possesses a more defined pore structure compared to T1, with a greater pore-filling capacity.

Figure 8B shows that composites T1 and T2 primarily contain mesopores (2-100 nm) rather than micropores (<2 nm). T1, however, has a higher pore count and volume than T2, consistent with the nitrogen adsorption-desorption isotherm data in Figure 8A. The greater pore size and volume in T1 indicate that CNCs treated with NaOH produce a more porous composite. This increased porosity is linked to the higher degree of crystallinity in the CNCs (Table 1). Furthermore, the enhanced porosity of composite T1 results in a larger surface area, as indicated in Table 3. This expanded surface area improves the composite's interaction with its environment, increasing sensitivity to ammonia vapor generated during fish spoilage. As a result, composite T1 is expected to be a more effective colorimetric indicator

for assessing fish freshness. Table 3 further confirms that the inclusion of CNCs as a filler significantly enhances the composite's surface area.

3.3. Response of Foam Biocomposites as Colorimetric Indicators

3.3.1. Response to Fish Freshness

Fish, a widely consumed source of animal protein, is highly susceptible to spoilage. The degradation of proteins in fish occurs due to microbial activity and natural enzymatic reactions, resulting in the production of ammonia and volatile amine compounds, which increase the pH level.

As packaged fish deteriorates, its pH rises to help consumers evaluate the freshness of fish, smart packaging can be employed, featuring a colorimetric indicator that changes color in response to spoilage levels. The specific pigments in the indicator determine the nature of the color change. These indicators effectively provide a visual representation of pH changes in the environment, making them valuable for monitoring fish freshness.

Figure 9 shows the response of T1, a colorimetric indicator, when applied to fresh Nile tilapia stored at 5°C for 30 days. The T1 composite, which incorporates anthocyanins from butterfly pea flowers, changes color from purple to green in reaction to pH variations. At pH 5, the anthocyanins shift to a blue-green hue due to the formation of quinonoidal bases [46]. This behavior aligns with previous research using butterfly pea flowers as colorimetric pigments [13,27,28,47]. The T1 indicator, which incorporates CNCs as a filler, demonstrates improved sensitivity in detecting pH changes due to the accumulation of total volatile basic nitrogen (TVBN) compared to previous colorimetric indicators that utilized cellulose fibers [28]. Previous indicators were unable to detect color changes at a TVBN level of 9-10 mg/100 g. In contrast, the T1 indicator effectively responded to a TVBN value of 7.13 mg/100 g by day 15 (Figure 10).

3.3.2. pH and Total Volatile Amine Analysis

The TVBN values for the fish samples on days 21 and 30 were 10.32 mg/100 g and 32.86 mg/100 g, respectively, indicating a significant decline in freshness. This finding corresponds with the noticeable color change to green in the colorimetric indicator observed on the same days. According to [48], Fish are deemed fresh when the Total Volatile Basic Nitrogen (TVBN) value is below 10 mg/100 g. Values exceeding 30 mg/100 g indicate that the fish is unfit for consumption. TVBN compounds, which are basic and volatile byproducts of protein breakdown, show a direct correlation between increases in TVBN levels and pH levels, as illustrated in Figure 10. Thus, TVBN values serve as a reliable indicator of fish freshness.

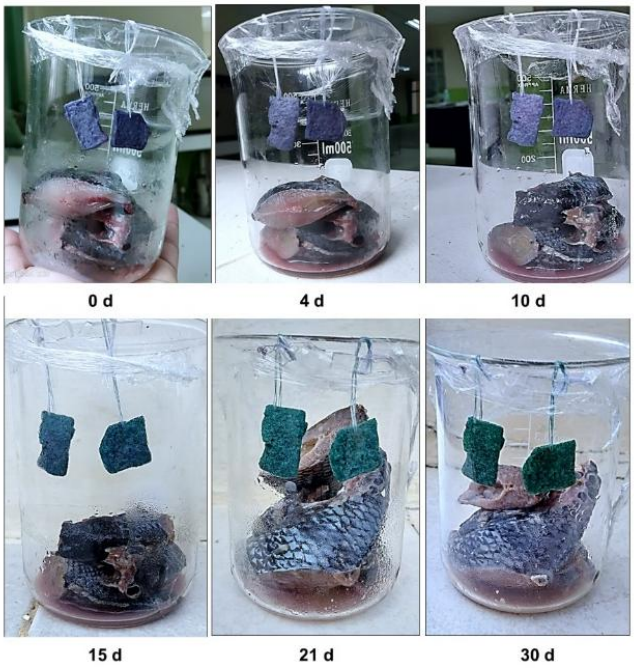

Fig. 9. Response of colorimetric indicator (BCF/CNCs-NaOH) to fish spoilage stored at 5°C for 30 days

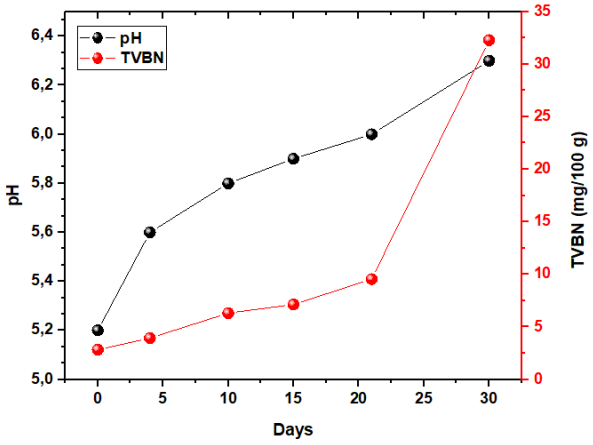

Fig. 10. Postmortem changes in pH and TVB-N in nile tilapia (*Oreochromis niloticus*) during storage at 5°C for 30 days

The results in Figure 10 indicate a significant increase in TVBN values after day 21 at a cold storage temperature of 5°C. Previous studies, such as [49] TVBN levels increase after 15 days of storage at 4°C. This study establishes a consistent correlation between the color changes observed in the T1 colorimetric indicator and the accumulation of TVBN and pH throughout the storage period. Consequently, the T1 composite, which is immobilized with anthocyanins from butterfly pea flowers, demonstrates significant potential for further development as a smart packaging solution for monitoring fish freshness.

At the start of the study, the TVBN value for fresh fish

was 2.83 mg/100 g. Over the subsequent five days of storage at 5°C, this value increased to 3.94 mg/100 g. By day 10, the TVBN value had risen to 6.31 mg/100 g, continuing to increase gradually to 7.13 mg/100 g and 10.32 mg/100 g on days 15 and 21, respectively. This gradual rise in TVBN values over 21 days indicates a decline in fish quality, although the fish remained safe for consumption during this period. However, by day 30, the TVBN value sharply increased to 32.86 mg/100 g, indicating rancidity. This significant rise in TVBN correlates with the development of a strong fishy odor, rendering the fish unfit for consumption.

4. Conclusions

This study successfully demonstrated that the type of alkali agent used during the delignification process significantly influences the physicochemical properties of cellulose nanocrystals (CNCs) isolated from the stem bark of *Calotropis gigantea.* Delignification with NaOH produced CNCs with the highest crystallinity index (89.54%) and a uniform, needle-like, and glossy morphology. In contrast, CNCs obtained from Na_2SO_3 treatment exhibited lower crystallinity (51.11%) and an agglomerated, irregular particle structure. CNCs-NaOH exhibited superior reinforcing performance when applied in biocomposite foams (BCFs), resulting in a porous structure with a high specific surface area (10.64 m^2/g), which enabled the effective immobilization of pH-sensitive anthocyanin dyes extracted from *Clitoria ternatea*.

The application of CNCs-NaOH-reinforced BCFs as colorimetric indicators for monitoring the freshness of *Oreochromis niloticus* at 5 °C for 30 days showed significant and linear color changes in response to increasing pH levels (from 5.2 to 6.3) and total volatile base nitrogen (TVB-N) content (from 2.83 to 32.86 mg/100 g). These findings confirm the high sensitivity and responsiveness of the developed indicator in detecting fish spoilage in a real-time and non-destructive manner.

Overall, this study introduces a novel approach to utilizing *Calotropis gigantea*, an underutilized lignocellulosic biomass, as an alternative cellulose source for CNC production. The results highlight the effectiveness of NaOH-treated CNCs as functional fillers in porous smart packaging materials designed for food quality monitoring. This research addresses a crucial scientific gap in optimizing local biomass resources for intelligent packaging technologies while offering a practical and eco-friendly solution for real-time seafood freshness monitoring.

Acknowledgments

This project was funded by the Ministry of Education, Research, and Technology of the Republic of Indonesia through the Doctoral Dissertation Research Grant (PDD) scheme No.611/UN11.2.1/PG.01.03/SPK/DRTPM/2024.

References

[1] R. C. Nagarajarao, Recent advances in processing and packaging of fishery products: A review. *Aquat. Procedia*, 7 (2016) 201–213.

[2] A. Mardhiah, M. Musran, L. Handayani, Intelligent packaging dalam perspektif filsafat ilmu. *J. Sains Riset*, 13 (2023) 125–133.

[3] F. Ebrahimi Tirtashi, M. Moradi, H. Tajik, M. Forough, P. Ezati, B. Kuswandi, Cellulose/chitosan pH-responsive indicator incorporated with carrot anthocyanins for intelligent food packaging. *Int. J. Biol. Macromol.*, 136 (2019) 920–926.

[4] S. Mohammadalinejhad, H. Almasi, M. Moradi, Immobilization of Echium amoenum anthocyanins into bacterial cellulose film: A novel colorimetric pH indicator for freshness/spoilage monitoring of shrimp. *Food Control*, 113 (2020) 107169.

[5] B. Merz, C. Capello, G. C. Leandro, D. E. Moritz, A. R. Monteiro, G. A. Valencia, A novel colorimetric indicator film based on chitosan, polyvinyl alcohol and anthocyanins from jambolan (Syzygium cumini) fruit for monitoring shrimp freshness. *Int. J. Biol. Macromol.*, 153 (2020) 625–632.

[6] S. Pourjavaher, H. Almasi, S. Meshkini, S. Pirsa, E. Parandi, Development of a colorimetric pH indicator based on bacterial cellulose nanofibers and red cabbage (Brassica oleraceae) extract. *Carbohydr. Polym.*, 156 (2017) 193–201.

[7] B. Kuswandi, Jayus, A. Restyana, A. Abdullah, L. Y. Heng, M. Ahmad, A novel colorimetric food package label for fish spoilage based on polyaniline film. *Food Control*, 25 (2012) 184–189.

[8] P. Özkaya, S. Dağbağlı, Usage of natural colour indicators in packaging materials for monitorization of meat freshness. *Turk. J. Agric. Food Sci. Technol.*, 9 (2021) 1869–1875.

[9] P. Ezati, H. Tajik, M. Moradi, R. Molaei, Intelligent pH-sensitive indicator based on starch-cellulose and alizarin dye to track freshness of rainbow trout fillet. *Int. J. Biol. Macromol.*, 132 (2019) 157–165.

[10] A. Nurfawaidi, B. Kuswandi, L. Wulandari, Pengembangan label pintar untuk indikator kesegaran daging sapi pada kemasan. *e-J. Pustaka Kesehatan*, 6 (2018) 199–204.

[11] J. Zhang, X. Zou, X. Zhai, X. W. Huang, C. Jiang, M. Holmes, Preparation of an intelligent pH film based on biodegradable polymers and roselle anthocyanins for monitoring pork freshness. *Food Chem.*, 272 (2019) 306–312.

[12] J. Liu, H. Wang, M. Guo, L. Li, M. Chen, S. Jiang, X. Li, S. Jiang, Extract from Lycium ruthenicum Murr. incorporating κ-carrageenan colorimetric film with a wide pH–sensing range for food freshness monitoring. *Food Hydrocoll.*, 94 (2019) 1–10.

[13] J. Zia, G. Mancini, M. Bustreo, A. Zych, R. Donno, A. Athanassiou, D. Fragouli, Porous pH natural indicators for acidic and basic vapor sensing. *Chem. Eng. J.*, 403 (2021) 126373.

[14] J. Han, Y. Yue, Q. Wu, C. Huang, H. Pan, X. Zhan, C. Mei, X. Xu, Effects of nanocellulose on the structure and properties of poly(vinyl alcohol)-borax hybrid foams. *Cellulose*, 24 (2017) 4433–4448.
[15] A. Lakshumu Naidu, S. Kona, Experimental study of the mechanical properties of banana fiber and groundnut shell ash reinforced epoxy hybrid composite. *Int. J. Eng., Trans. A: Basics*, 31 (2018) 659–665.
[16] B. Y. Mekonnen, Y. J. Mamo, Tensile and flexural analysis of a hybrid bamboo/jute fiber-reinforced composite with polyester matrix as a sustainable green material for wind turbine blades. *Int. J. Eng., Trans. B: Appl.*, 33 (2020) 314–319.
[17] K. Sumada, P. Erka Tamara, F. Alqani, Isolation study of efficient α-cellulose from waste plant stem Manihot Esculenta crantz. *J. Tek. Kim.*, 5 (2011) 434–438.
[18] H. Chen, *Biotechnology of Lignocellulose: Theory and Practice*. Springer, Dordrecht (2014). https://doi.org/10.1007/978-94-007-6898-7
[19] S. Muhammad, R. D. Bairwan, H. P. S. A. Khalil, M. Marwan, M. I. Ahmad, C. K. Abdullah, Comparative study of lignin from patchouli waste fibers and spent coffee grounds as biofillers in poly(3-hydroxybutyrate-co-3-hydroxyvalerate)-based biodegradable packaging materials. *Bioresour. Technol. Rep.*, 30 (2025) 101991.
[20] M. Iqbal, S. Rizal, R. D. Bairwan, I. Zein, H. P. S. Abdul Khalil, Enhanced biodegradable packaging composites: Performance of poly(3-hydroxybutyrate-co-3-hydroxyvalerate) (PHBV) reinforced with propionylated abaca fiber mats. *Polym. Compos.*, 46 (2025) 275-285.
[21] S. F. A. Karim, M. N. A. Azmi, N. A. Razak, S. A. Adnan, F. Mulana, Antibacterial and antioxidant performance of thermoplastic starch/polyethylene active film packaging through the incorporation of Aloe Vera gel. *Chem. Eng. Trans.*, 112 (2024) 235–240.
[22] Rahmi, A. Patra, Lelifajri, Fabrication of coconut dregs residue derived nano-cellulose film for food packaging. *S. Afr. J. Chem. Eng.*, 48 (2024) 71–79.
[23] A. A. Kacaribu, R. Rahmi, J. Julinawati, H. Fathana, M. Reza, M. Iqhramullah, Preparation and characterization of cellulose film from velvet tamarind rind (Dialium indum L.) for food packaging. *Appl. Sci. Eng. Prog.*, 18 (2025) 7724.
[24] S. Maji, R. Mehrotra, S. Mehrotra, Extraction of high quality cellulose from the stem of Calotropis procera. *S. Asian J. Exp. Biol.*, 3 (2013) 113–118.
[25] N. Reddy, Y. Yang, Extraction and characterization of natural cellulose fibers from common milkweed stems. *Polym. Eng. Sci.*, 49 (2009) 2212–2217. https://doi.org/10.1002/pen.21469
[26] K. Song, X. Zhu, W. Zhu, X. Li, Preparation and characterization of cellulose nanocrystal extracted from Calotropis procera biomass. *Bioresour. Bioprocess.*, 6 (2019) 39.
[27] L. Handayani, S. Aprilia, N. Arahman, M. R. Bilad, Assessment of fibers from different part of the Calotropis gigantea biomass as a filler of composites foam PVA/PVP. *S. Afr. J. Chem. Eng.*, 49 (2024) 189–198.
[28] L. Handayani, S. Aprilia, N. Arahman, M. R. Bilad, Identification of the anthocyanin profile from butterfly pea (Clitoria ternatea L.) flowers under varying extraction conditions: Evaluating its potential as a natural blue food colorant and its application as a colorimetric indicator. *S. Afr. J. Chem. Eng.*, 49 (2024) 151–161.
[29] N. Huda, J. Roslan, Isolation and characterization of nanocrystalline cellulose isolated from pineapple crown leaf fiber agricultural wastes using acid hydrolysis. *Polymers*, 13 (2021) 3591.
[30] A. A. Oun, J. Rhim, Characterization of nanocelluloses isolated from Ushar (Calotropis procera) seed fiber: Effect of isolation method. *Mater. Lett.*, 168 (2016) 146–150. https://doi.org/10.1016/j.matlet.2016.01.052
[31] K. Yoganandam, P. Ganeshan, B. NagarajaGanesh, K. Raja, Characterization studies on Calotropis procera fibers and their performance as reinforcements in epoxy matrix. *J. Nat. Fibers*, 17 (2020) 1706–1718.
[32] P. Narayanasamy, P. Balasundar, S. Senthil, M. R. Sanjay, S. Siengchin, A. Khan, A. M. Asiri, Characterization of a novel natural cellulosic fiber from Calotropis gigantea fruit bunch for ecofriendly polymer composites. *Int. J. Biol. Macromol.*, 150 (2020) 793–801.
[33] T. W. Kurniawan, H. Sulistyarti, B. Rumhayati, A. Sabarudin, Combination of the alkali-bleaching-sodium sulfite ionic solutions treatment toward cellulose isolation and its characteristics from palm empty bunches (PEB) (Study: Comparison with cellulose from different biomass and methods). *Moroc. J. Chem.*, 12 (2024) 21–42.
[34] R. Ramasamy, K. Obi Reddy, A. Varada Rajulu, Extraction and characterization of Calotropis gigantea bast fibers as novel reinforcement for composites materials. *J. Nat. Fibers*, 15 (2018) 527–538.
[35] M. G. Serna-Diaz, A. Arana-Cuenca, J. Medina-Marin, J. C. Seck-Tuoh-Mora, Y. Mercado-Flores, A. Jiménez-González, A. Téllez-Jurado, Modeling of sulfite concentration, particle size, and reaction time in lignosulfonate production from barley straw using response surface methodology and artificial neural network. *BioResources*, 11 (2016) 9219–9230.
[36] E. Hermawan, Pembuatan partikel selulosa menggunakan larutan alkalin. *J. Tek. Mesin (JTM)*, 6 (2017) 56–61.
[37] H. Wang, N. Chen, F. Xie, E. Verkasalo, J. Chu, Structural properties and hydrolysability of paulownia elongate: The effects of pretreatment methods based on acetic acid and its combination with sodium sulfite or sodium sulfite. *Int. J. Mol. Sci.*, 23 (2022) 5775.
[38] M. O. Ichwan, A. J. Onyianta, R. S. Trask, A. Etale, S. J. Eichhorn, Production and characterization of cellulose nanocrystals of different allomorphs from oil palm empty fruit bunches for enhancing composite interlaminar fracture toughness. *Carbohydr. Polym. Technol. Appl.*, 5 (2023) 100272.
[39] R. M. Braga, T. R. Costa, J. C. O. Freitas, J. M. F. Barros, D. M. A. Melo, M. A. F. Melo, Pyrolysis kinetics of elephant grass pretreated biomasses. *J. Therm. Anal. Calorim.*, 117 (2014) 1341–1348.
[40] E. U. P. Barragán, C. F. C. Guerrero, A. M. Z. Cepeda, A. B. M. Heinze, T. Heinze, A. Koschella, Isolation of cellulose nanocrystals from Typha domingensis named Southern Cattail using a batch reactor. *Fibers Polym.*, 20 (2019) 1136–1144.
[41] V. Fiore, T. Scalici, A. Valenza, Characterization of a new natural fiber from Arundo donax L. as potential reinforcement of polymer composites. *Carbohydr. Polym.*, 106 (2014) 77–83.

[42] M. K. Herliansyah, N. Nurbaiti, A. E. Tontowi, M. G. Widiastuti, H. V. Hoten, Effect of adding nanocrystalline cellulose on reducing micro-crack of three-dimensional printed hydroxyapatite/collagen composite. *Int. J. Eng., Trans. B: Appl.*, 38 (2025) 2537–2546.

[43] L. Ding, X. Han, L. Cao, Y. Chen, Z. Ling, J. Han, S. He, S. Jiang, Characterization of natural fiber from manau rattan (Calamus manan) as a potential reinforcement for polymer-based composites. *J. Bioresour. Bioprod.*, 7 (2022) 190–200. https://doi.org/10.1016/j.jobab.2021.11.002

[44] X. Y. Tan, S. B. Abd Hamid, C. W. Lai, Preparation of high crystallinity cellulose nanocrystals (CNCs) by ionic liquid solvolysis. *Biomass Bioenergy*, 81 (2015) 584–591.

[45] F. Jiang, Y. L. Hsieh, Chemically and mechanically isolated nanocellulose and their self-assembled structures. *Carbohydr. Polym.*, 95 (2013) 32–40.

[46] L. Handayani, S. Aprilia, N. Arahman, M. R. Bilad, Anthocyanin extraction and pH-modulated color alterations in butterfly pea flower (Clitoria ternatea L.). In: *IOP Conf. Ser.: Earth Environ. Sci.*, Vol. 1359, IOP Publishing, Bogor (2024) 012087.

[47] S. Rawdkuen, A. Faseha, S. Benjakul, P. Kaewprachu, Application of anthocyanin as a color indicator in gelatin films. *Food Biosci.*, 36 (2020) 100603.

[48] L. Farber, Freshness test. In: *Fish as Food*, Vol. IV, G. Borgstrom (Ed.), Academic Press, New York (1965) 65-126.

[49] A. E. D. A. Bekhit, B. W. B. Holman, S. G. Giteru, D. L. Hopkins, Total volatile basic nitrogen (TVB-N) and its role in meat spoilage: A review. *Trends Food Sci. Technol.*, 109 (2021) 280–302.